Scientia Iranica C (2015) 22(6), 2341–2349

SCIENTIA
IRANICA

Sharif University of Technology
Scientia Iranica
Transactions C: Chemistry and Chemical Engineering
www.scientiairanica.com

Pd/$La_xSr_{1x}FeO_3$ perovskite nanocatalysts for selective catalytic reduction of NO_x by hydrogen

A. Nemati[a], **A.A. Khodadadi**[a,b], **Y. Mortazavi**[a,b,*] and **A. Alinezhadchamazketi**[a]

a. *Catalysis and Nanostructured Materials Laboratory, School of Chemical Engineering, College of Engineering, University of Tehran, Tehran, P.O. Box 11155/4563, Iran.*
b. *Oil and Gas Processing Center of Excellence, College of Engineering, University of Tehran, Tehran, P.O. Box 11155/4563, Iran.*

Received 25 August 2014; received in revised form 3 May 2015; accepted 5 September 2015

KEYWORDS
Hydrogen;
NO;
Palladium;
Perovskite;
Selective catalytic reduction.

Abstract. In this study, $La_xSr_{1-x}FeO_3$ ($x = 0$, 0.8) perovskite-type catalysts were prepared by gel combustion method and then 1.0 wt% palladium was loaded on them by a dry impregnation. The catalysts were characterized by XRD, SEM, H_2-TPR, O_2-TPD, NO-TPD, and BET surface area techniques. H_2-TPR profiles of the Pd/perovskite catalyst show reduction of Pd at around 140°C which facilitates the reduction of NO in H_2-SCR. TPD results reveal that substitution of Sr in the perovskites structure remarkably decreases the oxygen mobility and increases the NO adsorption. The H_2-SCR of NO on the catalysts was performed in a temperature-programmed reaction apparatus in the presence of oxygen. The effect of carbon monoxide in the feed on H_2-SCR was also investigated. The PLSFO catalyst (1.0 wt% Pd/$La_{0.8}Sr_{0.2}FeO_3$) shows the highest NO conversion and N_2 selectivity at a moderate temperature of 190 °C.

1. Introduction

Nitrogen oxide is a hazardous pollutant in the exhaust of diesel engines. Selective Catalytic Reduction (SCR) of NO_x by reducing agents in presence of oxygen is one of the important methods for NO_x removal from the exhaust gas. Ammonia (NH_3-SCR) and hydrocarbons (HC-SCR) are currently used as the reducing agents for NO_x removal [1-3]. However, there is a great concern about increasing the carbon dioxide emissions in environment and problems related to the use of NH_3 as a reducing agent, e.g. NH_3 slip [1] and distribution of ammonia [4].

Nowadays, development of green technologies that lead to reduction in CO_2 and NO_x require suitable non-carbon-containing reducing agents for removal of NO_x from exhaust gas streams. Hydrogen, as a green reducing agent, has been studied for the selective catalytic reduction of NO in presence of oxygen (H_2-SCR). Using hydrogen as a reducing agent in SCR-systems for NO_x-removal lead to NO_x-reduction to low temperatures (e.g. below 200-300°C) under oxygen-rich conditions, wherein the traditional reducing agents fail to function properly. The main challenge is N_2 selectivity at low temperatures without producing large amounts of N_2O [5].

Three following main reactions occur during the reduction of NO_x in excess oxygen environments by adding H_2 as a reducing agent [5]. Reaction (1) leads to reduction of NO to form N_2; in Reaction (2) N_2O is formed; and in Reaction (3) H_2 is oxidized and H_2O is generated:

$$2NO + 4H_2 + O_2 \rightarrow N_2 + 4H_2O, \qquad (1)$$

$$2NO + 3H_2 + O_2 \rightarrow N_2O + 3H_2O, \qquad (2)$$

$$O_2 + 2H_2 \rightarrow 2H_2O. \qquad (3)$$

Since N_2O contributes more to the greenhouse effect

---

[*] *Corresponding author. Tel./Fax: +98 21 6696 7793*
E-mail address: mortazav@ut.ac.ir (Y. Mortazavi)

compared to CO_2, Reaction (2) must be impeded [5]. Therefore, the development of catalysts with high N_2 selectivity is of a great interest.

Supported platinum catalysts have been found as the most active catalysts for the H_2-SCR reaction at low temperatures ($T < 200°C$) [6-9]. Yokota et al. [6] have reported catalytic results for this process over Pt-Mo-Na/SiO_2 catalyst, and Costa et al. [7,8] have investigated the $NO/H_2/O_2$ reaction over the Pt/MgO-CeO_2 catalyst. These two catalysts have the highest N_2 selectivity of about 75%, as compared to the conventional supported Pt catalysts (e.g., Pt/Al_2O_3 and Pt/SiO_2). It has been also reported that in presence of water, Pt-Mo-Na/SiO_2 catalyst shows a relatively low stability under H_2-SCR conditions [6]. Frank et al. [9] studied kinetics of the $NO/H_2/O_2$ reaction over Pt-Mo-Co/α-Al_2O_3 catalyst. They showed that hydrogen promotes dissociation of NO by decreasing the NO coverage. However, high coverage of H_{ad} reduces the likelihood of two N_{ad}s to recombine and decreases the reaction rate of NO_x reduction decreases. Furthermore, the significant effect of nitrate formation on NO conversion at low temperatures has been reported by Machida and co-workers [10]. They reported that the reduced catalyst exhibits a much higher activity for NO reduction than the oxidized catalyst. On the reduced catalyst, nitrate should be formed from NO and O_2 that chemisorbed onto Pt particles. In contrast, the oxidized catalyst may produce nitrate via direct reactions between NO and oxidized Pt surface.

Perovskite type catalysts for H_2-SCR have been studied in the last decade. Costa et al. studied Pt/$La_{0.7}Sr_{0.2}Ce_{0.1}FeO_3$ [11] and Pt/$La_{0.5}Ce_{0.5}MnO_3$ [12] for this process. These two catalysts exhibited remarkable activity and N_2 selectivity. However, the former catalyst had greater operating temperature windows compared to the latter one. According to their work, the presence of oxygen vacancies in the perovskite structure plays an effective role for NO adsorption and dissociation. Furfori et al. [13] studied the presence of Sr, Ce, and Pd in $LaFeO_3$ perovskite structure. The formation of anion vacancies in presence of Sr had a better effect on the catalytic activity than the formation of cation vacancies in presence of Ce. Deposition of Pd onto the catalyst increased the catalytic activity because of the enhanced H_2 chemisorption function of palladium. Furthermore, some other formulations of the perovskite such as $BaTi_{0.95}Pd_{0.05}O_3$ [5] were studied for H_2-SCR process. It was found that the presence of H_2O vapor and CO_2 had a positive effect on the $NO/O_2/H_2$ reaction and the presence of CO in the gas mixture caused a poisonous effect on the NO_x-conversion and N_2-selectivity.

In this study, $La_xSr_{1-x}FeO_3$ ($x = 0, 0.8$) perovskites and the ones containing 1.0 wt% Pd are synthesized, characterized, and tested for $NO/H_2/O_2$ lean de-NO_x reaction. The effects of CO in the feed gas mixture are also investigated.

2. Experimental

2.1. Catalyst preparation

Perovskite catalysts were prepared by a gel combustion method. Aqueous solutions of $La(NO_3)_3.6H_2O$, $Fe(NO_3)_3.9H_2O$, $Sr(NO_3)_2$ (all from Merck) as precursors, and sorbitol ($C_6H_{14}O_6$, Merck) as the fuel, in a stoichiometric ratio, were used for the synthesis. Sorbitol plays a double role in the synthesis; it reacts with the precursors (metal nitrates) and by forming complexes with metal cations in aqueous solution, facilitates solution homogeneity. The proper amounts of the precursors and the fuel (cations:sorbitol molar ratio for LFO was 0.866 and Fe/La/Sr:sorbitol molar ratios for LSFO were 0.903, 0.722 and 0.18, respectively) were dissolved in distilled water and the resulting solution, stirred thoroughly to ensure complete dissolution of all the reagents, was transferred into a ceramic dish and placed in a microwave oven. Following the evaporation of water, a significant increase in viscosity and temperature of the sample occurred and finally a spongy powder was formed. The powder was calcined at 600°C in air for 5h. The gel combustion synthesis procedure can be simply explained in the following steps (preparation of lanthanum ferrite is considered here as an example):

$$La(NO_3)_3+Fe(NO_3)_3 \rightarrow LaFeO_3 + 3N_2+7.5O_2, \quad (4)$$

$$C_6H_{14}O_6 + 6.5O_2 \rightarrow 6CO_2 + 7H_2O. \quad (5)$$

The first reaction is endothermic and represents the perovskite synthesis, while the second one is highly exothermic and accounts for the reaction between the fuel (sorbitol) and oxygen derived from nitrate decomposition. Some direct combustion of sorbitol with atmospheric oxygen cannot be excluded as the reaction is carried out in air. The heat generated in the second reaction compensates for the first endothermic reaction. Thus, gel combustion method is considered as a self-sustained synthesis method. Finally, Pd is deposited on the perovskite via dry impregnation with an aqueous solution of $Pd(NO_3)_2.2H_2O$ (from Merck). The prepared powder was dried in an oven at 120°C for 12 h and then calcined in air at 500°C for 5 h, in order to decompose the nitrate and obtain small and well dispersed palladium clusters over the perovskite surface. Hereafter, the catalysts are represented by short forms which are shown in Table 1.

2.2. Catalyst characterization

The crystal structures of the catalysts were determined by X-ray powder diffraction (XRD) with a Bruker AXD8 diffractometer using Cu-Kα radiation. Field

Table 1. Acronyms for the catalysts names.

Catalyst	Acronyms
$LaFeO_3$	LFO
$La_{0.8}Sr_{0.2}FeO_3$	LSFO
1%wt Pd/ $La_{0.8}Sr_{0.2}FeO_3$	PLSFO

Emission Scanning Electron Microscopy (FESEM) was done by a Philips XL30 instrument to determine the particle size and morphology as well as the elemental composition of catalysts.

BET, H_2-temperature programmed reduction (H_2-TPR), and O_2-temperature programmed desorption (O_2-TPD) experiments were carried out using a Quantachrome CHEMBET-3000 apparatus. BET specific surface areas were measured at the liquid nitrogen temperature by N_2 adsorption.

The H_2-TPR experiments were performed on 15 mg of each catalyst placed in a U-shaped quartz reactor. Prior to each TPR run, the catalyst was degassed in a flow of 10 sccm Ar at 300°C for 1 h and cooled down to room temperature under the same atmosphere. Then the sample reduced in 7.0% H_2/Ar mixture by 10 sccm while the temperature raised to 950°C with a heating rate of 10°C/min.

The O_2-TPD experiment was performed on 15 mg of each perovskite sample placed in a U-shaped quartz reactor. Prior to each TPD run, the catalyst was degassed in air atmosphere similar to H_2-TPR experiments. After a 1h exposure to air flow at 300°C, the reactor was cooled down to room temperature by keeping the same flow rate of air, thereby allowing a fully oxidized catalyst with adsorbed oxygen over its surface. Helium was then fed to the reactor at 10 sccm flow rate for 30 min at room temperature in order to purge any excess oxygen molecules of the catalyst surface. The catalyst was then heated to 500°C at a constant heating rate of 10°C/min under a flow of 10 sccm of helium.

NO Temperature Programmed Desorption (NO-TPD) experiments were carried out using a Bruker VECTOR 22 FTIR apparatus. The experiments were performed on 20 mg of perovskite samples in a quartz reactor. Prior to each NO-TPD run, the catalyst was heated in 10 sccm helium to 300°C, remained at this temperature for 1 h, and cooled down to room temperature by keeping the same flow rate of helium. The sample was then exposed to 10 sccm of a mixture of 2500 ppm NO in He, followed by switching the flow to pure helium for 5 min at room temperature in order to purge any excess NO molecules of the catalyst surface. The catalyst was then heated to 500°C at a constant heating rate of 10°C/min under a flow of 10 sccm of helium. The NO desorbed during the heating was detected by FTIR equipped with a 1.5 cm ID and 7.0 cm long (10 mL) gas cell.

2.3. Catalytic activity measurement

A gas mixture of 1000 ppm NO, 1.0 vol% H_2, and 5.0 vol% O_2 in Ar was used as a synthetic exhaust gas of diesel engines. 100 sccm of the gas mixture was set by a mass flow controller. Furthermore, 5000 ppm CO was added to the gas mixture for investigation of NO conversion in the presence of CO.

Conversion of the synthetic exhaust gas pollutants was investigated in a fixed bed microreactor at atmospheric pressure. All the catalyst samples were pelleted, crushed, and sieved to the particle size of 0.125-0.297 mm (50-120 mesh size). 100 mg of each sample, supported by a small amount of quartz wool, was used to measure the catalysts activity. A thermocouple, placed inside the catalyst bed, was used for both monitoring and controlling temperature of the reactor. Samples were heated from ambient temperature up to 450°C under the reaction atmosphere and after that steady state condition was achieved at the desired temperature, concentration of the effluents (i.e. NO and N_2O) was analyzed on-line with the FTIR.

Processing of the results was made by applying the following equations:

NO_x-conversion to N_2 and N_2O:

$$X=\frac{[NO_{x_{\mathrm{in}}}]-[NO_{x_{\mathrm{out}}}]}{[NO_{x_{\mathrm{in}}}]}\times\%100. \quad (6)$$

Selectivity to N_2:

$$S_{N_2}=\frac{[NO_{x_{\mathrm{in}}}]-[NO_{x_{\mathrm{out}}}]-2\,[N_2O]}{[NO_{x_{\mathrm{in}}}]-NO_{x_{\mathrm{out}}}}\times\%100. \quad (7)$$

3. Results and discussion

3.1. XRD, BET, and SEM characterization results

The XRD spectra and crystal structures of LFO and LSFO perovskite catalysts, calcined at 600°C for 5h, are presented in Figure 1 and Table 2, respectively. All samples have the perovskite structures and the dominant crystal structure of LFO is cubic (JCPDS card: PDF 01-074-2203 for LFO). In the case of LFO samples, by partial substitution of La with Sr, the structure becomes more asymmetric and changes from cubic to orthorhombic (JCPDS card: PDF 00-035-1480 for LSFO). In the XRD patterns of LSFO and PLSFO catalysts, a diffraction peak is observed at around $2\theta = 39.8°$ and 52.7° which corresponds to the presence of PdO (JCPDS card: PDF 00-085-0713) and SrO phase (JCPDS card: PDF 00-027-1304), respectively. However, the peaks are not clearly resolved probably due to the low concentration of Pd and Sr in the samples and their overlaps with the main perovskite peak.

The crystallite sizes of the catalysts (d_{XRD}) were calculated from XRD using the Debye-Scherrer equa-

Table 2. Summary of catalyst characterization results, XRD and BET specific surface area.

Catalyst	**Peak index (h k l)**	**Average crystallite size, d_{XRD} (nm)**	**Crystal structures**	**BET surface area ($\mathrm{m^2/g}$)**	**Average particle size, d_{BET} (nm)**	**$d_{\mathrm{BET}}/d_{\mathrm{XRD}}$**
LFO	(1 1 0)	48	Cubic	19	54	1.1
LSFO	(0 2 0)	60	Orthorhombic	16	70	1.2

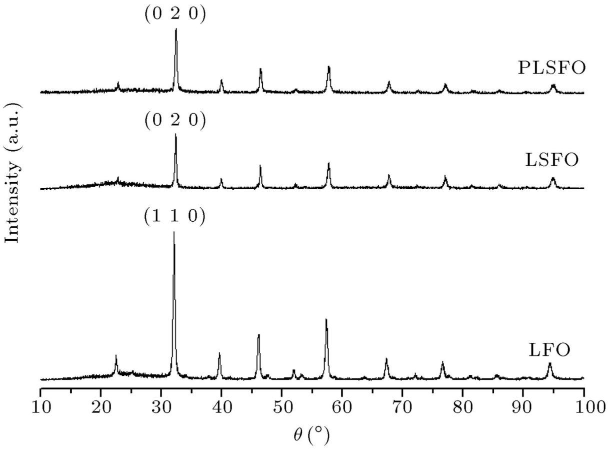

Figure 1. XRD patterns of LFO, LSFO, and PLSFO catalysts calcined at 600°C for 5 h.

tion:

$$d = \frac{0.9\lambda}{\beta.\cos\theta}, \tag{8}$$

where d is the crystallite size, λ is the wavelength of Cu-Kα radiation, β is the peak width at the half maximum of (1 1 0) and (0 2 0) planes for LFO and LSFO/PLSFO, respectively, and θ is the Bragg diffraction angle. The calculated crystallite sizes are presented in Table 2. By adding strontium to the LFO catalyst, the crystallite size increases (Table 2).

The BET Specific Surface Area (SSA) of the catalysts is also reported in Table 2. Adding strontium to the samples reduces the SSA values. In addition, considering the spherical loose particles, the BET average particle sizes (d_{BET}) are estimated using the equation d=6000/($\rho\times S_{\mathrm{BET}}$), where S_{BET} is BET surface area in $\mathrm{m^2/g}$ and ρ is the skeletal density in $\mathrm{g/cm^3}$. Then, the ratio of $d_{\mathrm{BET}}/d_{\mathrm{XRD}}$, as an indication of degree of nanoparticles aggregation [14], is calculated for each sample. As the degree of aggregation increases during the calcination, the specific surface area decreases.

Figure 2 presents the SEM micrographs of the LSFO catalyst. It has been reported that during the combustion synthesis, the decomposition/combustion of precursors and fuel generate a large amount of gaseous products in a short period of time. This leads to a spongy morphology [15]. The SEM micrographs (Figure 2) show that the perovskite particles are agglomerated to some extent.

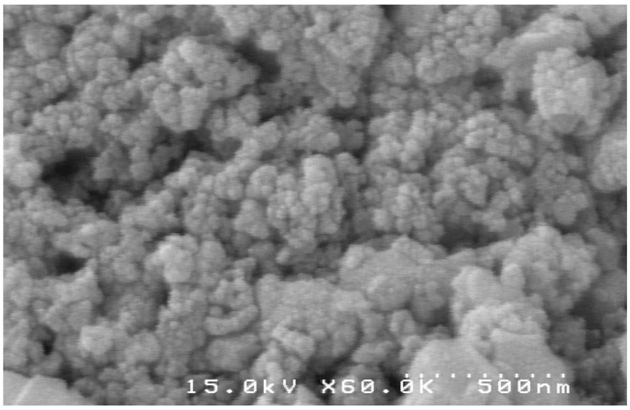

Figure 2. SEM micrographs of the LSFO sample.

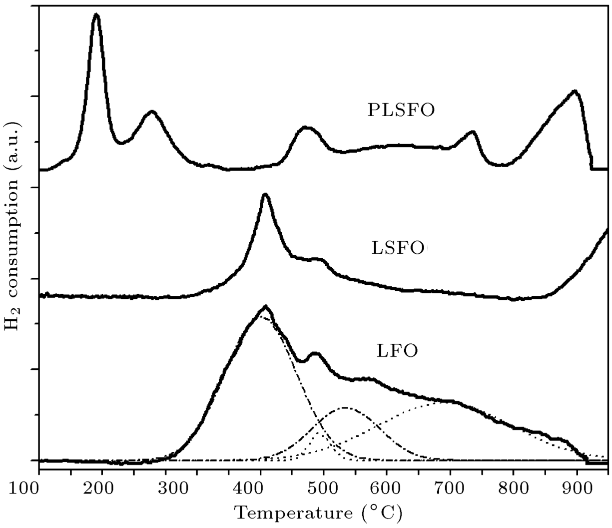

Figure 3. TPR profile of LFO, LSFO, and PLSFO catalysts by 10 sccm of 7% H_2/Ar mixture, 10°C/min from 50 to 950°C.

3.2. H_2 temperature programmed reduction

Reducibility of the catalyst samples was studied by H_2-TPR experiments, as shown in Figure 3. The amount of H_2 uptake was calculated by deconvolution of the H_2-TPR peaks via Gaussian peak fitting and is reported in Table 3. TPR profiles of the sample provide useful information about reducibility of the Fe^{n+} species in the LFO and LSFO mixed oxides, since the La^{3+} and Sr^{2+} are both non-reducible under the reductive atmosphere [16]. For the LFO perovskite, four reduction peaks are detected at 410, 490, 580, and 720°C (Figure 3). The first two peaks attribute

Table 3. H_2 uptake of catalysts in H_2-TPR.

Catalyst	**H_2 uptake (mmol H_2/g catalyst) $T < 600$°C**
LFO	1.5
LSFO	0.46
PLSFO	0.77

to the reduction of Fe^{3+} to Fe^{2+} occurring over the surface and in bulk of $LaFeO_3$, respectively, while the others are ascribed to the reduction of Fe^{2+} to metallic iron occurring over the surface and in bulk of $LaFeO_3$, respectively [17,18].

Adding Strontium to the LFO catalyst decreases the reducibility of catalyst significantly (Table 3). In presence of Strontium, the catalyst structure changes from cubic to orthorhombic (Table 2) and becomes more asymmetric. This phenomenon causes a lower mobility of oxygen in the catalyst bulk, resulting in lower reducibility of the catalyst. Furthermore, the presence of Sr shifts the reduction peak of Fe^{2+} to higher temperatures. For the PLSFO catalyst (Figure 3), the first reduction peak at 140°C attributes to reduction of Pd^{2+} to Pd^0 and highly reducible Fe^{4+} ions [17,19]. In presence of Pd, reduction peak of surface Fe^{3+} shifts to much lower temperatures. This may indicate that the Pd clusters are located on the surface of catalyst.

3.3. O_2 temperature programmed desorption

Mobility of oxygen for the calcined catalysts was investigated by O_2-TPD experiment in the range of reaction temperatures, as illustrated in Figure 4. Two types of oxygen species are distinguished in a TPD profile: the α-type oxygen, which is ascribed to the adsorbed oxygen bound to the surface anion vacancies usually desorbed in the 300-700°C range, and the β-type oxygen attributed to those oxygen species usually liberated from the lattice at above 700°C [15,17]. According to the previous repor [15], the onset and the intensity of α-oxygen peak depend partially on the nature of the metal B in the ABO_3 structure, but mainly on the degree of substitution of the A ion with ions of lower valence. Figure 4 shows that by adding Sr to the samples, the amounts of α-oxygen desorption reduce in Fe containing perovskites. It may suggest that Sr ions occupy some of the surface vacancies in Fe containing perovskites, which results in a decrease of α-oxygen. Furthermore, in presence of Sr, oxygen mobility probably reduces because the catalyst structure becomes more asymmetric (Table 2).

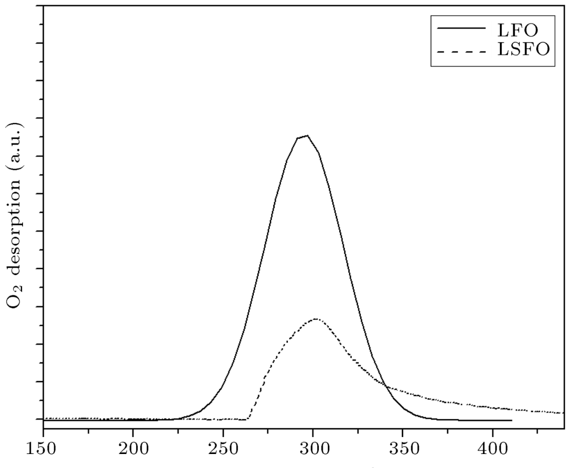

Figure 4. O_2-TPD profifiles of LFO and LSFO catalysts in 10 sccm He; 10°C/min from 100 to 500°C.

3.4. NO temperature programmed desorption

Figure 5 presents the thermal desorption patterns of the catalyst samples. Presence of strontium and palladium increases the adsorption of nitrous oxide on LSFO and PLSFO catalysts. Maximum NO desorption occurred at temperatures greater than 300°C. The large activity of Pd and Fe for NO oxidation by interaction between NO and surface oxygen anions could lead to the production of nitrite and nitrate species that adsorb on the catalyst via the following routes [20]:

$$\text{Nitrites: } ``\mathrm{M-O{-}N{-}O \rightarrow M{+}NO{+}1/2O_2''}. \tag{9}$$

$$\text{Mono- or bi-dentate nitrates: } ``\mathrm{M-O-NO_2}$$

$$\text{or } \mathrm{M-O-(NO)-O-M \rightarrow M+NO+O_2''}. \tag{10}$$

Basic sites of strontium have the ability to adsorb nitrite and nitrate species; furthermore, lanthanum ions facilitate the adsorption of nitrites [20].

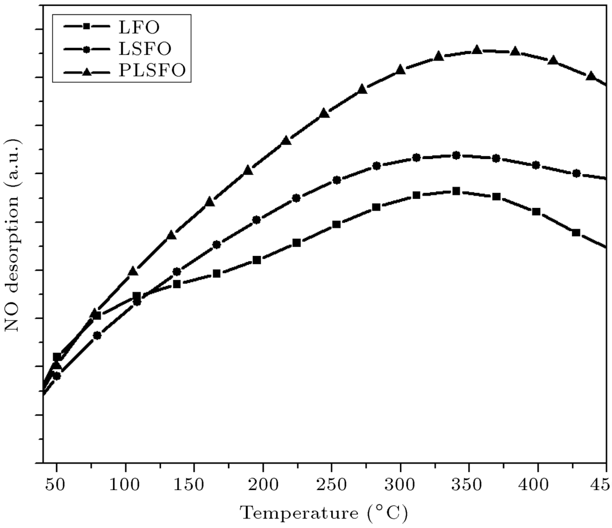

Figure 5. NO-TPD profiles of Fe containing catalysts in 10 sccm of He; 10°C/min from 40 to 450°C.

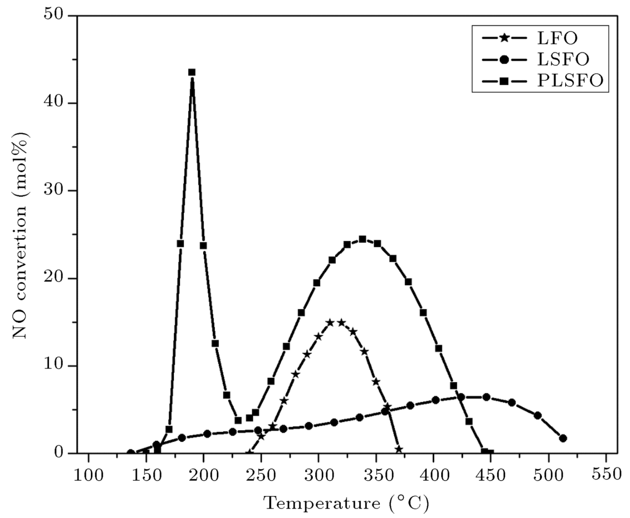

Figure 6. NO conversion of perovskite catalysts; 0.1 g catalyst and 100 sccm feed flow.

Palladium could adsorb NO in two ways; first by nitrosyl groups (Pd-NO^+) and second by the help of oxygen vacant sites. Oxygen vacancies of support located next to the small Pd clusters could provide the means for formation of adsorbed NO with *N* atom located on the Pd metal and the O atom on the oxygen vacant sites [11].

3.5. Catalytic activity results

Catalytic activities for perovskite catalysts without Pd are shown in Figure 6. Adding strontium to the LFO catalyst increases the ability of catalysts for NO conversion. The catalysts show the maximum NO desorption at temperatures higher than 300°C (Figure 5). Therefore, these supports may adsorb NO at low temperatures as nitrite and nitrate species which results in reduction of these species at high temperatures in presence of hydrogen. For LSFO, two peaks are observed for NO conversion. The first peak is related to the reduction of nitrite species desorbed at lower temperatures and the second peak is related to the reduction of nitrate species.

LSFO perovskite support shows higher activity for NO reduction by hydrogen in presence of oxygen; therefore we impregnated palladium onto this support and used it for NO reduction. PLSFO catalyst shows NO conversion peak at low temperature ranges, and higher NO conversion at high temperature ranges, in comparison with the corresponding LSFO without Pd. The appearance of two maxima in the temperature profile of NO conversion on the Pd-containing catalyst is based on the bifunctionality of the catalyst. The Pd metal operates at the low temperature range, while the perovskites operate in the range of 250-500°C.

At low temperatures, hydrogen is dissociatively adsorbed on the palladium. Hydrogen atoms can reduce nitrosyl groups or can move toward the metal-support interfaces and reduce NO molecules adsorbed on oxygen vacant sites. This may be presented schematically in Figure 7.

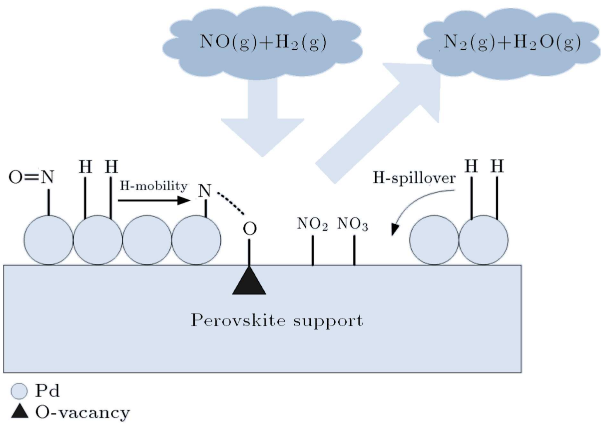

Figure 7. Reduction process of NO by hydrogen dissociative adsorption on Pd.

General mechanism for H_2-SCR has been suggested based on the following elementary reactions [11,12]:

$$H_2(g) + 2s \rightarrow H - s + H - s, \tag{11}$$

$$O_2(g) + 2s \rightarrow O - s + O - s, \tag{12}$$

$$NO(g) + s \rightarrow NO - s, \tag{13}$$

$$NO - s + s \rightarrow N - s + O - s, \tag{14}$$

$$N - s + N - s \rightarrow N_2(g) + 2s, \tag{15}$$

$$NO - s + N - s \rightarrow N_2O(g) + 2s, \tag{16}$$

$$NO - s + H - s \rightarrow N - s + OH - s, \tag{17}$$

$$OH - s + H - s \rightarrow H_2O(g) + 2s. \tag{18}$$

Reaction (12) in this mechanism hinders NO reduction, since the strong dissociatively-adsorbed oxygen blocks most active sites for hydrogen dissociation. Furthermore, formation of hydrogen and nitrogen atoms has an effective role in the H- and N-assisted dissociation of nitrogen oxides adsorbed molecularly on palladium clusters, respectively [11,12]. Reaction (17) shows a H-assisted NO dissociation mechanism, while N-assisted NO reduction to N_2 or N_2O is shown in Reactions (15) and (16). In addition, Reactions (15) and (16) show that when NO absorbed molecularly onto the catalyst, N_2O was produced; however, dissociative adsorbed NO results in production of more N_2 [11,12,20].

At high temperature ranges, nitrite and nitrate species reduce by hydrogen. As mentioned earlier, NO conversion increases in presence of palladium at high

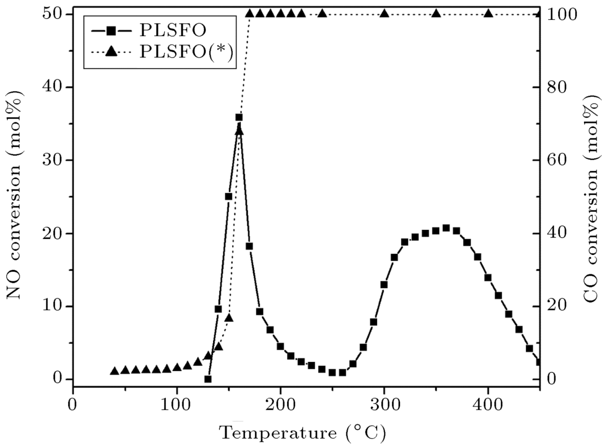

Figure 8. Effect of CO on H_2-SCR process; (*) for CO conversion to CO_2.

temperatures. The main reason for this phenomenon is hydrogen spillover from palladium to perovskite support [20], as illustrated in Figure 7.

The effect of CO on H_2-SCR was also investigated. NO conversion and CO conversion to CO_2 are presented in Figure 8. In presence of CO, NO conversion decreases and Pd containing catalyst shows high activity for CO conversion to CO_2. Since carbon monoxide is known to block active Pd sites at low temperatures and it decreases catalysts activity [21], CO should be removed before the H_2-SCR catalyst. This goal may be achieved by using a Diesel Oxidation Catalyst (DOC) prior to the H_2-SCR catalyst. DOC system is a state-of-the-art technology and is applied to oxidize CO and HC in diesel vehicles [22].

N_2 selectivity of the catalysts is shown in Figure 9. Perovskites, due to their oxygen deficiency, can cause the dissociation of both NO molecules and hydrogen. H-assisted NO dissociation phenomenon could lead to more N_2 production. Therefore, all the catalysts show more than 70% selectivity to N_2. As is shown in Figure 9, presence of palladium reduces the N_2 selectivity. This may indicate that a series of perovskite active sites for NO dissociation are blocked by Pd clusters.

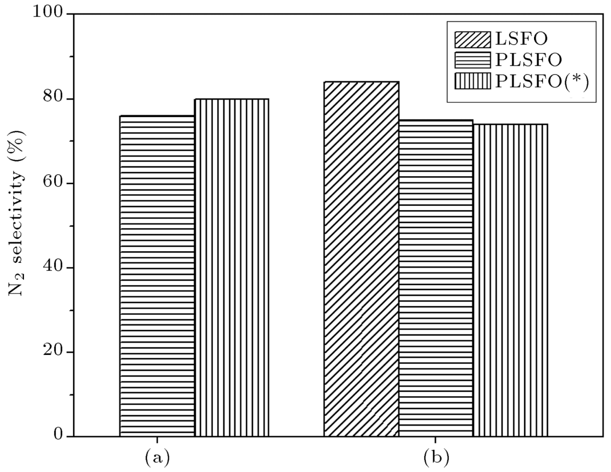

Figure 9. N_2 selectivity of catalysts: (a) At maximum NO conversion at low temperatures; and (b) at maximum NO conversion at high temperatures, (*) in the presence of CO.

4. Conclusion

$LaFeO_3$ and $La_{0.8}Sr_{0.2}FeO_3$ perovskites prepared by gel combustion synthesis and the ones impregnated by 1.0wt% Pd were used for selective catalytic reduction of NO by H_2 in the presence of oxygen. The Pd containing catalysts were active in two temperature ranges. In the low temperature range, Pd-NO species and NO molecules which are adsorbed on the oxygen vacant sites of the perovskites might reduce, while at the high temperature ranges, reduction of nitrite and nitrate species, which are formed in presence of Pd and stored on the surface of perovskites, occur. The Pd-containing catalyst also showed higher NO conversion at high temperature range. The 1.0 %wt Pd/$La_{0.8}Sr_{0.2}FeO_3$ exhibited the highest catalytic activity for H_2-deNO_x process with more than 75% N_2 selectivity. More adsorbed NO on the Sr-containing catalyst increases NO conversion in the high temperature range. In presence of CO in the feed gas mixture, NO conversion decreases at both low and high temperature ranges and all the catalysts showed high N_2 selectivity, probably due to large ability of these catalysts for NO dissociation.

References

1. Roy, S., Hegde, M.S. and Madras, G. "Catalysis for NO_x abatement", *Applied Energy*, **86**, pp. 2283-2297 (2009).

2. Shelef, M. "Selective catalytic reduction of NO_x with N-free reductants", *Chemical Reviews*, **95**, pp. 209-225 (1995).

3. Skalska, K., Miller, J.S. and Ledakowicz, S. "Trends in NOx abatement: A review", *Science of the Total Environment*, **408**, pp. 3976-3989 (2010).

4. Parvulescua, V.I., Grangeb, P. and Delmon, B. "Catalytic removal of NO", *Catalysis Today*, **46**, pp. 233-316 (1998).

5. Mondragón Rodríguez, G.C., Kelm, K. and Saruhan, B. "H_2-selective catalytic reduction of NO_x activity and microstructural analysis of new $BaTi_{0.95}Pd_{0.05}O_3$ catalyst", *Applied Catalysis A: General*, **387**, pp. 173-184 (2010).

6. Yokota, K., Fukui, M. and Tanaka, T. "Catalytic removal of nitric oxide with hydrogen and carbon

monoxide in the presence of excess oxygen", *Applied Surface Science*, **121/122**, pp. 273-277 (1997).

7. Costa, C.N. and Efstathiou, A.M. "Pt/Mg-Ce-O catalyst for NO/H_2/O_2 lean de-NO_x reaction", *Environ. Chem. Lett.*, **2**, pp. 55-58 (2004).
8. Costa, C.N., Savva, P.G., Fierro, J.L.G. and Efstathiou, A.M. "Industrial H_2-SCR of NO on a novel Pt/MgO-CeO_2 catalyst", *Applied Catalysis B: Environmental*, **75**, pp. 147-156 (2007).
9. Frank, B., Emig, G. and Renken, A. "Kinetics and mechanism of the reduction of nitric oxides by H_2 under lean-burn conditions on a Pt-Mo-Co/α-Al_2O_3 catalyst", *Applied Catalysis B: Environmental*, **19**, pp. 45-57 (1998).
10. Machida, M., Ikeda, S., Kurogi, D. and Kijima, T. "Low temperature catalytic NO_x-H_2 reactions over Pt/TiO_2-ZrO_2 in an excess oxygen", *Applied Catalysis B: Environmental*, **35**, pp. 107-115 (2001).
11. Costa, C.N., Savva, P.G., Andronikou, C., Lambrou, P.S., Polychronopoulou, K., Belessi, V.C., Stathopoulos, V.N., Pomonis, P.J. and Efstathiou, A.M. "An investigation of the NO/H_2/O_2 (lean de-NO_x) reaction on a highly active and selective Pt/$La_{0.7}Sr_{0.2}Ce_{0.1}FeO_3$ catalyst at low temperatures", *Journal of Catalysis*, **209**, pp. 456-471 (2002).
12. Costa, C.N., Stathopoulos, V.N., Belessi, V.C. and Efstathiou, A.M. "An investigation of the NO/H_2/O_2 (lean-deNO_x) reaction on a highly active and selective Pt/$La_{0.5}Ce_{0.5}MnO_3$ catalyst", *Journal of Catalysis*, **197**, pp. 350-364 (2001).
13. Furfori, S., Bensaid, S., Russo, N. and Fino, D. "Towards practical application of lanthanum ferrite catalysts for NO reduction with H_2", *Chemical Engineering Journal*, **154**, pp. 348-354 (2009).
14. Habibzadeh, S., Khodadadi, A.A. and Mortazavi, Y. "CO and ethanol dual selective sensor of Sm_2O_3-doped SnO_2 nanoparticles synthesized by microwave-induced combustion", *Sensor and Actuators B*, **144**, pp. 131-138 (2010).
15. Fino, D., Russo, N., Saracco, G. and Specchia, V. "The role of suprafacial oxygen in some perovskites for the catalytic combustion of soot", *Journal of Catalysis*, **217**, pp. 367-375 (2003).
16. Zhong, H. and Zeng, R. "Structure of $LaSrMO_4$ (M = Mn, Fe, Co, Ni, Cu) and their catalytic properties in the total oxidation of hexane", *Journal of the Serbian Chemical Society*, **71**(10), pp. 1049-1059 (2006).
17. Zhang, R., Villanueva, A., Alamdari, H. and Kaliaguine, S. "Cu- and Pd-substituted nanoscale Fe-based perovskites for selective catalytic reduction of NO by propene", *Journal of Catalysis*, **237**, pp. 368-380 (2006).
18. Levasseur, B. and Kaliaguine, S. "Effects of iron and cerium in $La_{1-y}Ce_yCo_{1-x}Fe_xO_3$perovskites as catalysts for VOC oxidation", *Applied Catalysis B: Environmental*, **88**, pp. 305-314 (2009).
19. Kumar, M.S., Eyssler, A., Hug, P., van Vegten, N., Baiker, A., Weidenkaff, A. and Ferri, D. "Elucidationof structure-activity relationships of model three way catalysts for the combustion of methane", *Applied Catalysis B: Environmental*, **94**, pp. 77-84 (2010).
20. Chiarello, G.L., Ferri, D., Grunwaldt, J.D., Forni, L. and Baiker, A. "Flame-synthesized $LaCoO_3$-supported Pd, 2. Catalytic behavior in the reduction of NO by H_2 under lean conditions", *Journal of Catalysis*, **252**, pp. 137-147 (2007).
21. Schott, F.J.P., Balle, P., Adler, J. and Kureti, S. "Reduction of NO_x by H_2 on Pt/WO_3/ZrO_2 catalysts in oxygen-rich exhaust", *Applied Catalysis B: Environmental*, **87**, pp. 18-29 (2009).
22. Ponce, S., Peña, M.A. and Fierro, J.L.G. "Surface properties and catalytic performance in methane combustion of Sr-substituted lanthanum manganites", *Applied Catalysis B: Environmental*, **24**, pp. 193-205 (2000).

Biographies

Ahmad Nemati received the BSc degree in Chemical Engineering from the University of Mazandaran and the MSc degree in Chemical Engineering from University of Tehran in 2012. He has been a research assistant at Catalysis and Nanostructured Materials Research Laboratory, University of Tehran, since 2010. His research interests include synthesis and characterization of nanostructured materials and their environmental effects.

Abbas Ali Khodadadi received his MSc in Chemical Engineering from University of Tehran in 1986 and his PhD in Catalysis and Reaction Engineering from University of Waterloo, Canada, in 1994. His research interests include synthesis of nanostructured materials including metals (oxides), carbon nanotubes, graphene, etc. via various methods and their application in nano/bio/photo/plasma-catalytic reactions, gas/biosensing, and nano-filters and membranes for natural gas and petroleum conversions and air pollution control.

Yadollah Mortazavi received the BSc degree in Chemical Engineering from University of Shiraz, Shiraz, Iran, and the MSc and PhD degrees in Chemical Engineering from University of Waterloo, Waterloo, Ontario, Canada. He joined as faculty member to University of Tehran in 1995 and is currently chairman of Nanotechnology Department at the College of Engineering, University of Tehran, Tehran, Iran. His research interests include catalysis and reaction engineering, especially in C1 chemistry, air pollution control, chemical gas sensors, and nanostructured materials.

Ali Alinezhadchamazketi received the BSc degree in Chemical Engineering from Isfahan University of Technology and the MSc degree in Chemical Engineering from University of Tehran in 2012. He has been a research assistant at Catalysis and Nanostructured Materials Research Laboratory, University of Tehran, since 2010. His research interests include synthesis and characterization of nanostructured materials and their environmental effects.